Nogo-A/NgR signaling regulates stemness in cancer stem-like cells derived from U87MG glioblastoma cells

CHENGJIN AI[1*], YU ZHOU[1*], KUNMING PU[2], YI YANG[3] and YINGYING ZHOU[4]

[1]Department of Laboratory Medicine, Hospital of Chengdu University of Traditional Chinese Medicine; [2]Department of Ultrasound, The Second People's Hospital of Chengdu, Chengdu, Sichuan 610072; [3]Department of Ultrasound, Chengdu Women's and Children's Central Hospital, School of Medicine, University of Electronic and Technology of China, Chengdu, Sichuan 611731; [4]Hospital of Chengdu University of Traditional Chinese Medicine, Chengdu, Sichuan 610072, P.R. China

Received January 8, 2022; Accepted March 28, 2022

DOI: 10.3892/ol.2022.13351

Abstract. Neurite outgrowth inhibitor A (Nogo-A), a member of the reticulon 4 family, is an axon regeneration inhibitor that is negatively associated with the malignancy of oligodendroglial tumors. It has been suggested that the Nogo-A/Nogo Receptor (NgR) pathway plays a promoting effect in regulating cancer stem-like cells (CSCs) derived from glioblastoma, indicating that Nogo-A could exert different roles in CSCs than those in parental cancer cells. In the present study, CSCs were generated from the human Uppsala 87 malignant glioma (U87MG) cell line. These U87MG-CSCs were characterized by the upregulation of CD44 and CD133, which are two markers of stemness. The expression levels of Nogo-A and the differentiation of U87MG-CSCs were investigated. In addition, the proliferation, invasion and colony formation U87MG-CSCs were examined. Using culture in serum-containing medium, U87MG-CSCs were differentiated into neuron-like cells specifically expressing MAP2, β-III-tubulin and nestin. Nogo-A was upregulated in U87MG-CSCs compared with parental cells. Knockdown of Nogo-A and inhibition of the Nogo-A/NgR signaling pathway in U87MG-CSCs markedly decreased cell viability, cell cycle entry, invasion and tumor formation, indicating that Nogo-A could regulate U87MG-CSC function. Moreover, Nogo-A was involved in intracellular ATP synthesis and scavenging of accumulated reactive oxygen species. Nogo-A/NgR pathway exerted protective effects against hypoxia-induced non-apoptotic and apoptotic cell death. These results suggest that Nogo-A plays an important role in regulating U87MG-CSCs via the Nogo-A/NgR signaling pathway. Nogo-A may also different roles in U87MG-CSCs compared with their parental cells.

Correspondence to: Professor Yingying Zhou, Hospital of Chengdu University of Traditional Chinese Medicine, 37 Shi-er-qiao Road, Jinniu, Chengdu, Sichuan 610072, P.R. China
E-mail: 513148252@qq.com

*Contributed equally

Key words: Nogo-A, glioblastoma, cancer stem-like cells, malignancy, apoptosis

Introduction

Glioblastoma is one of the most prevalent and aggressive primary type of brain tumor and is associated with high morbidity and mortality (1). At present, surgery, chemotherapy, and radiation are the most common therapeutic approaches for cancer treatment. However, the prognosis of malignant glioma remains poor, with recurrence and low survival times (2,3). Recently, it has been reported that a sub-population of cells, namely cancer stem-like cells (CSCs), contributes to poor prognosis by inducing chemoresistance, radioresistance and recurrence (4,5). CD133, CD44 and CD24 are stem cell surface markers expressed in different types of cancer, but their expression and distribution differ between cancer types and tumor cell lines (6). Therefore, the identification of CSCs through these biomarkers is of great interest.

Nogo-A functions as a growth-inhibitory, antiadhesive, and growth cone-collapsing factor in neurons and has a high molecular weight (7). In the adult central nervous system (CNS), Nogo-A exerts repulsive and guidance functions for neurite development (8), inhibits the movement of cells in the early stage of development (9), and functions as an inhibitor for axonal regeneration and plasticity after development (10). Despite its functions in the CNS, Nogo-A is also known to exert regulatory roles in tumors. In oligodendroglial tumors, Nogo-A has been negatively associated with the malignancy grade (11). Schwab *et al* (12) suggested that, in neuroepithelial tumors, the expression levels of Nogo-A were positively associated with poor prognosis. A contrasting report has also shown that different expression levels of Nogo-A have no independent prognostic impact in glioblastoma, despite age and clinical status (13). Thus, the exact role of Nogo-A in glioblastoma and CSCs remains largely unclear.

In the present study, Nogo-A was upregulated in CSCs derived from the human Uppsala 87 malignant glioma cell line (U87MG-CSCs) compared with their parental cells. In contrast

to its effect in neurons, Nogo-A promoted the proliferation, invasion and tumor formation of U87MG-CSCs. These results suggested that Nogo-A may serve multiple functions and could represent a promising therapeutic target.

Materials and methods

Cell culture. U87MG glioblastoma cells of unknown origin (accession number, CVCL_0022) were obtained from the Cell Bank of Chinese Academy of Sciences (Shanghai, China) and maintained in Dulbecco's Modified Eagle Medium (DMEM; HyClone Laboratories, Inc.) with 10% fetal bovine serum (FBS Gibco; Thermo Fisher Scientific, Inc.) at 37˚C in a humidified atmosphere of 5% CO_2.

The CSCs were derived from U87MG cells by culturing parental cells in a serum-free DMEM/F12 medium (Gibco; Thermo Fisher Scientific, Inc.) supplemented with B-27 (20 mg/ml; Thermo Fisher Scientific, Inc.) which is an optimized serum substitute, 20 ng/ml basic fibroblast growth factor (bFGF; MilliporeSigma), 20 ng/ml epidermal growth factor (EGF; PeproTech, Inc.) at 37˚C as previously reported (14). The medium was half-refreshed every 3 days. The primary tumor spheres were detected within 10-14 days and subsequently dissociated and passaged in fresh medium every 2-3 days.

For the hypoxia experiments, the cells were initially maintained in 20% O_2 and 5% CO_2 (normoxia) at 37˚C, then placed in an incubator (H35 Hypoxystation, Don Whitley Scientific) with a gas mixture containing 1% O_2 and 5% CO_2 (hypoxia) at 37˚C. Culture media were kept in hypoxystation for 24 h before use.

GEPIA analysis of gene expression. GEPIA (gepia.cancer-pku.cn/index.html) is based on RNA sequences from Genotype Tissue Expression (GTEx) data and The Cancer Genome Atlas (TCGA) programs, including 9,736 cancer and 8,587 normal samples. In the present study, GEPIA was used to explore the mRNA expression level of Nogo-A in different kinds of cancer compared to adjacent tissues.

Colony formation assay. For colony formation, cells were plated at final concentration of $1x10^3$ cells/well and cultured in serum-free DMEM/F12 medium supplemented with 2% B-27, 20 ng/ml EGF and 20 ng/ml bFGF. The medium was half-replaced every three days. After 14 days, cells were then washed with PBS, fixed with 4% paraformaldehyde in PBS at room temperature for 10 min, stained with 0.1% crystal violet (MilliporeSigma) at room temperature for 10 min, washed with PBS, and the colonies >50 μm in diameter were counted under a X71 (U-RFL-T) fluorescence microscope (Olympus Corporation).

To block the Nogo-A/Nogo-A receptor (NgR) interaction, NEP1-40 (Cat. No.: HY-P1242, MedChemExpress, United States), a competitive antagonist of Nogo/NgR signaling pathway, was added into culture medium at a final concentration of 100 μg/ml at 37˚C for 24 h, while saline was used as a mock control.

Western blotting. Total protein extraction from U87MG and U87MG-CSCs was performed using the SoniConvert® Tissue-Cell Convertor (DocSense) and Animal Tissue/cells/bacteria total protein isolation kit (cat. no. PP001; DocSense, Chengdu, China) following the manufacturer's instruction. The protein concentration was measured using the Pierce BCA protein assay kit (Thermo Fisher Scientific, Inc.). Total protein samples (10 μg) were separated using 10% SDS-PAGE, then transferred onto a nitrocellulose membrane. After transferring, the membrane was blocked with PBS supplemented with 0.25% Tween 20 (PBS-T) and 5% skimmed milk for 1 h at room temperature. Following blocking, membranes were incubated for 1 h at room temperature with the following primary antibodies: Anti-CD24 antibody diluted 1:1,000 (cat. no. ab202073), anti-CD44 antibody diluted 1:2,500 (cat. no. ab157107), anti-CD133 antibody diluted 1:1,000 (cat. no. ab226355), anti-microtubule associated protein 2 (MAP2) antibody diluted 1:1,000 (cat. no. ab183830), anti-β III tubulin antibody diluted 1:1,000 (cat. no. ab18207), anti-GFAP antibody diluted 1:1,500 (cat. no. ab7260), anti-nestin antibody diluted 1:1,000 (cat. no. ab105389) and anti-β-actin (loading control) antibody diluted 1:5,000 (cat. no. ab8226). All primary antibodies and secondary antibody were bought from Abcam. The membranes were washed three times with PBS-T, then incubated with HRP-labeled goat anti-mouse IgG antibody diluted in 1:5,000 (cat. no. ab97040) or goat anti-rabbit IgG antibody diluted in 1:5,000 (cat. no. ab7090) for 1 h at room temperature. The protein bands were then detected using SuperSignal Western Femto Maximum Sensitivity Substrate (Thermo Fisher Scientific, Inc.) and analyzed using Quantity One (version 4.6.9, Bio-Rad Laboratories, Inc.).

Cell counting kit 8 (CCK-8) assays. Proliferation was evaluated using Cell Counting Kit 8 (CCK-8) assays. Cells ($5x10^3$ cells/well) were plated into 24-well culture plates containing 500 μl DMEM/F12 medium supplemented with 2% B-27, 20 ng/ml EGF and 20 ng/ml bFGF. Cells were incubated for 1-2 h at 37˚C and 5% CO_2 CCK-8 reagent (10 μl/well; MilliporeSigma) following the manufacturer's instructions. The cell growth curves represent normalized mean optical density at 450 nm of three independent samples recorded on days 1 to 5.

Transwell assays. Cell culture matrix Matrigel (MilliporeSigma) was diluted 1:5 in DMEM/F12. An 80-μl volume of diluted Matrigel was added to the upper chambers of Transwell inserts for pre-coating at 37˚C in a 5% CO_2 incubator for 4 h. CSCs were made into single-cell suspension, resuspended in DMEM/F12, and plated into the upper chamber at a density of $5x10^3$ cells/well and cultured at 37˚C. DMEM/F12 (600 μl) supplemented with 20 ng/ml EGF, 20 ng/ml bFGF and 2% B-27 was added to the lower chamber. After 24-h incubation, cells on the lower side were fixed in 4% paraformaldehyde at room temperature for 10 min and stained with 0.25% crystal violet at room temperature for 15 min. The cells were counted in five random fields of view under a light microscope.

Immunofluorescence staining. Cells were fixed and permeabilized with 4% paraformaldehyde in 1X PBS containing 0.1% Triton X-100 for 10 min at room temperature and non-specific binding was blocked with 10% normal goat serum (Sigma) in 1X PBS for 1 h at room temperature. The cells were incubated with primary antibodies against anti-β III tubulin antibody

diluted 1:1,000 (cat. no. ab18207), anti-GFAP antibody diluted 1:1,500 (cat. no. ab7260), anti-nestin antibody diluted 1:1,000 (cat. no. ab105389) at room temperature for 1 h. The Alexa Fluor 488-conjugated secondary antibody (Cat. No.: ab150077) was then added at dilution of 1:1,000 and incubated for 1 h at room temperature. All primary antibodies and secondary antibody were bought from Abcam. The cells were mounted in Vectashield® (Vector Laboratories, Ltd.) with Hoechst 33342 and imaged under a X71 (U-RFL-T) fluorescence microscope (Olympus Corporation).

Transduction. The shRNA targeting Nogo-A mRNA (shCCDC88A; targeting sequence: 5'-AATGATTCCGAG GCAGATTAT-3') and the scrambled negative control shRNA (shScrambled; scrambled sequence: 5'-AACGAACGAGTA CCGTACACT-3') were designed and bought from Guangzhou RiboBio Co., Ltd. Both shRNAs were inserted into GV248 lentiviral vectors. For lentiviral packaging, the shNogo-A or shScrambled vector was co-transfected into 293T cells (Shanghai Institute of Biochemistry and Cell Biology) with packing vectors (pVSVG and psPAX2, Addgene) at equal amount (1.2 μg each plasmid) using Lipofectamine® 2000 (Thermo Fisher Scientific, Inc.) according to the manufacturer's protocol at 37˚C. The medium was replaced 4 h later. After 72 h of transfection, the medium were centrifuged at 12.000 g, 4˚C for 15 min, and supernatant was collected and filtered. To silence Nogo-A, CSCs derived from U87MG glioblastoma cells were transduced with lentivirus with a multiplicity of infection of 10 at 37˚C for 4 h, followed by the replacement of supernatant with regular medium. GFP-expressing cells were imaged using a fluorescence microscope (Olympus Corporation). Cells stably expressing shRNA were established by culture in the presence of 10 μg/ml puromycin for selection and 5 μg/ml puromycin was used for maintenance.

Cell cycle analysis. Cell cycle distribution was analyzed by quantifying DNA content. CSCs with Nogo-A knockdown were harvested, washed with ice-cold PBS, and fixed overnight at 4˚C with ice-cold 70% ethanol. The fixed cells were washed with PBS for three times and incubated with final concentration of 100 μg/ml RNase A and 40 μg/ml propidium iodide (PI; Beyotime) for 30 min in the dark. Cells were analyzed using the three-laser Navios cytometer (Beckman Coulter Inc.).

Tumor formation in soft agar. Cells ($5x10^3$) were seeded in 1 ml of 0.3% melted agar in DMEM/F12 containing 2% B27, 20 ng/ml of EGF, and 20 ng/ml of bFGF and plated in 6-well plate with 0.6% agar in the same medium at 37˚C. Two weeks later, colonies were stained with 10 mg/ml of nitro blue tetrazolium (Sigma-Aldrich; Merck KGaA) at 37˚C and scanned 4 h later with an Epson Perfection 3200 scanner.

ATP production. Cells ($1x10^6$) cells were plated in 6-well plates and allowed to adhere overnight. ATP Lite assay kit (cat. no. 6016943; PerkinElmer, Inc.) was used to measure ATP production following the manufacturer's instruction.

Reactive oxygen species (ROS) detection. Total intracellular ROS was measured by flow cytometry after dichlorofluorescein (DCF) oxidation assays (cat. no. D399; Thermofisher Scientific, Inc.). The intracellular ROS oxidizes the cleaved dichlorodihydrofluorescein diacetate (DCFH-DA) which enters into the cells. Target cells ($5x10^5$) were incubated with DCFH-DA (10 μM) for 1 h at 37˚C, followed by three washes with ice-cold PBS and ROS fluorescence was analyzed using a microplate reader (Sinergy H1; BioTek). The signal of DCFH in shScrambled group at 24 h time point was used for normalization.

Statistical analysis. All data are presented as mean ± SD. Statistical differences were assessed using unpaired Student's t-tests. One-way analysis of variance (ANOVA) was performed to compare two groups with one variable followed by Tukey's post hoc test using Prism 6 (GraphPad Software). $P<0.05$ was considered to indicate a statistically significant difference. All experiments were repeated three times.

Results

Enrichment and identification of CSCs from glioblastoma cells. To obtain CSCs from U87MG glioblastoma cells, U87MG cells were cultured in serum-free medium. After 14 days, spheres were imaged (Fig. 1A). Spheres formed and suspended in medium, whereas parental cells attached to bottom of well. Western blotting was then performed to detect CD44, CD24, and CD133, which are three CSC markers (15,16). On days 7 and 14, spheres cultured in serum-free medium presented a marked increase in CD44 and CD133 levels, but not in CD24 levels, compared with cells cultured in serum-containing medium (Fig. 1B). Passages 1 to 4 presented consistent self-renewal capacity, confirming the stemness of the U87MG-derived CSCs (Fig. 1C).

CCK-8 assays were performed to detect cell proliferation from day 1 to day 4. U87MG-CSCs presented increased proliferation compared with their parental cells (Fig. 2A). Transwell invasion and tumor formation assays in soft agar were performed. U87MG CSCs presented enhanced invasion and tumor formation compared to U87MG cells (Fig. 2B and C). To further confirm CSC differentiation, CSCs were cultured in medium supplemented with FBS for 5 or 10 days to promote differentiation. MAP2, β-III tubulin, GFAP and nestin, which are markers of CSC differentiation (6), were then detected using western blot analysis. As shown in Fig. 2D and E, MAP2, β-III tubulin, and GFAP levels were upregulated in CSCs after 5 and 10-day culture in medium supplemented with FBS, and these proteins were also imaged through immunofluorescence staining. These data indicated that CSCs were successfully enriched from U87MG cells. Furthermore, these results indicated that enriched CSCs from U87MG presented increased viability, invasion and tumor formation compared with the parental cells.

Nogo-A is upregulated in U87MG-CSCs. By considering that Nogo-A is critically involved in regulating physiological processes in glioblastoma cancer (17,18), the expression of Nogo-A was analyzed in several types of cancer using GEPIA (Gene Expression Profiling Interactive Analysis), a web server for cancer and normal gene expression profiling and interactive analyses (19). Despite the upregulation of Nogo-A in pancreatic adenocarcinoma, no evident differences were observed in Nogo-A expression between tumor and adjacent tissue,

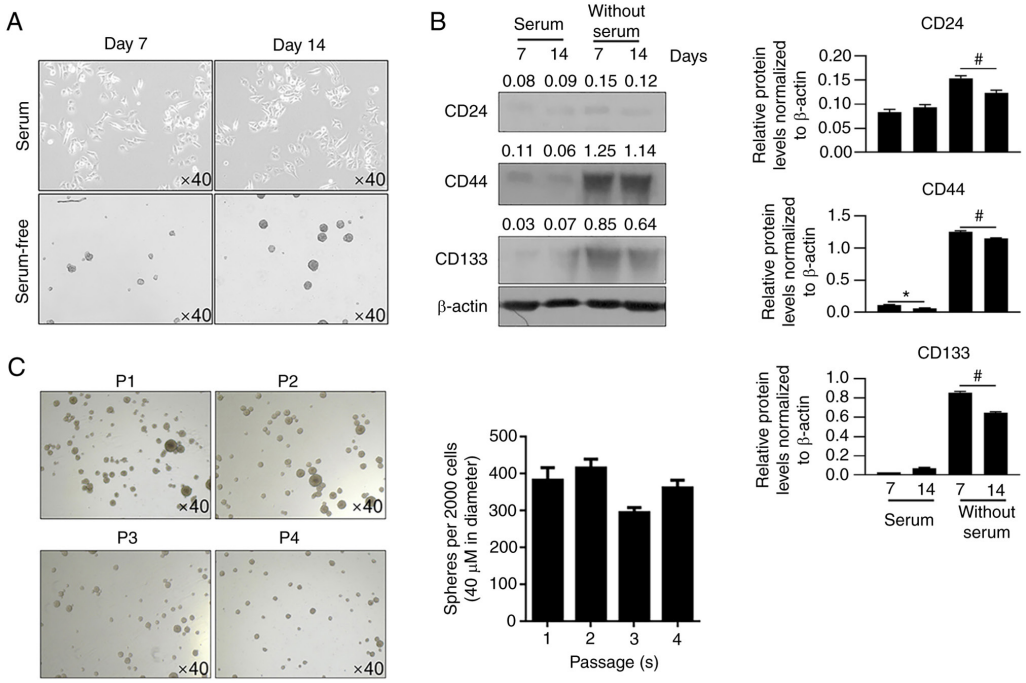

Figure 1. Generation and characterization of U87MG-CSCs. (A) After 7 and 14 days of culture with or without serum, cells were imaged. (B) Western blot analysis of CD24, CD44 and CD133 levels. *P<0.05 vs. 7 days with serum. #P<0.05 vs. 7 days without serum. (C) Serial replating assays were performed to detect the stemness of U87MG-CSCs. CSCs, cancer stem cells.

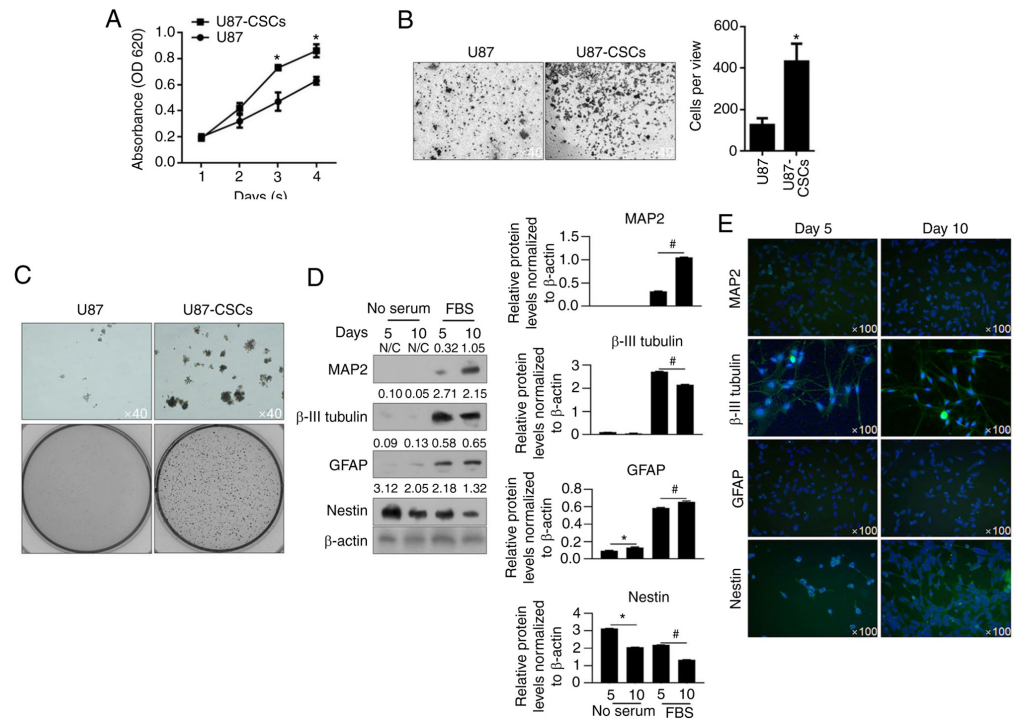

Figure 2. Proliferation, invasion and colony formation of U87 CSCs and its parental cells. (A) By performing CCK-8 assays, the proliferation of U87MG-CSCs from day 1 to 4 was measured. *P<0.05 vs. U87MG parental cells. (B) Transwell assays were performed to detect invasiveness of U87MG-CSCs. *P<0.05 vs. U87MG parental cells. (C) Tumor formation in soft agar was employed to detect the tumor formation in U87MG-CSCs compared to their parental cells. Upper lane, Magnification, x40; lower lane, imaged by digital camera. (D) To analyze differentiation, CSCs were cultured in FBS-supplemented medium for 5 and 10 days, then analyzed by western blotting. *P<0.05 vs. 5 days without serum; #P<0.05 vs. 5 days with serum. (E) Immunofluorescence staining of the neuronal markers, MAP2, β-III tubulin, GFAP and nestin. CCK-8, Cell Counting Kit-8; CSCs, cancer stem cells; MAP2, microtubule-associated protein 2; GFAP, glial fibrillary acidic protein; CSCs, cancer stem cells.

including in bladder urothelial carcinoma (BLCA), breast invasive carcinoma (BRCA), colon adenocarcinoma (COAD), kidney renal clear cell carcinoma (KIRC), lung adenocarcinoma (LUAD) and pancreatic adenocarcinoma (PAAD) (Fig. 3A).

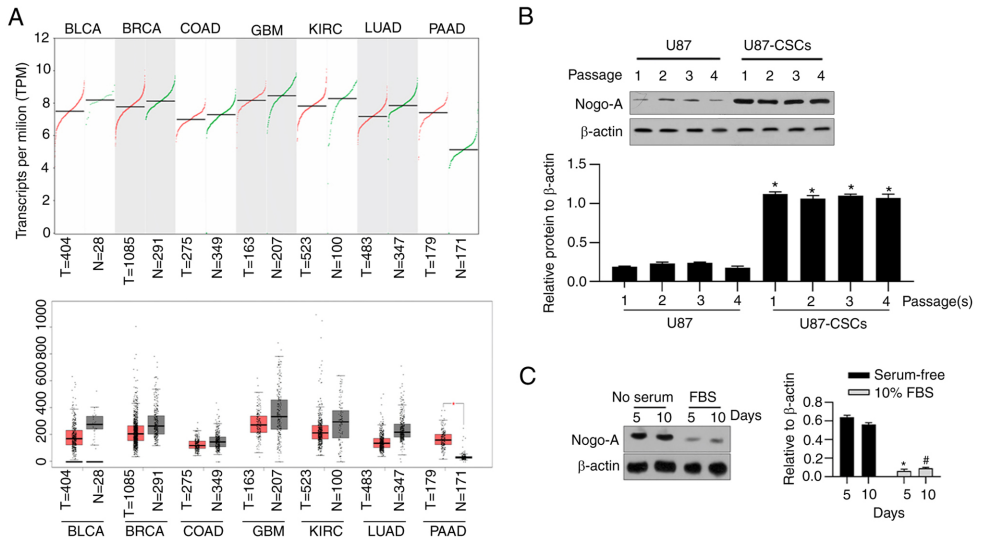

Figure 3. Nogo-A is upregulated in CSCs compared with parental cells. (A) Nogo-A expression was validated using GEPIA server (http://gepia.cancer-pku.cn/) in several type of cancer. (B) Western blotting was performed to detect Nogo-A in U87MG and U87MG-CSCs from passage 1 to 4. *P<0.05, vs. U87MG parental cells. (C) Western blotting was performed to detect Nogo-A after differentiation in serum-containing medium for 5 and 10 days. *P<0.05 vs. serum-free group; #P<0.05 vs. 10% FBS group. Nogo-A, neurite outgrowth inhibitor A; GEPIA, Gene Expression Profiling Interactive Analysis; Nogo-A, neurite outgrowth inhibitor A; CSCs, cancer stem cells; BRCA, breast invasive carcinoma; BLCA, bladder urothelial carcinoma.

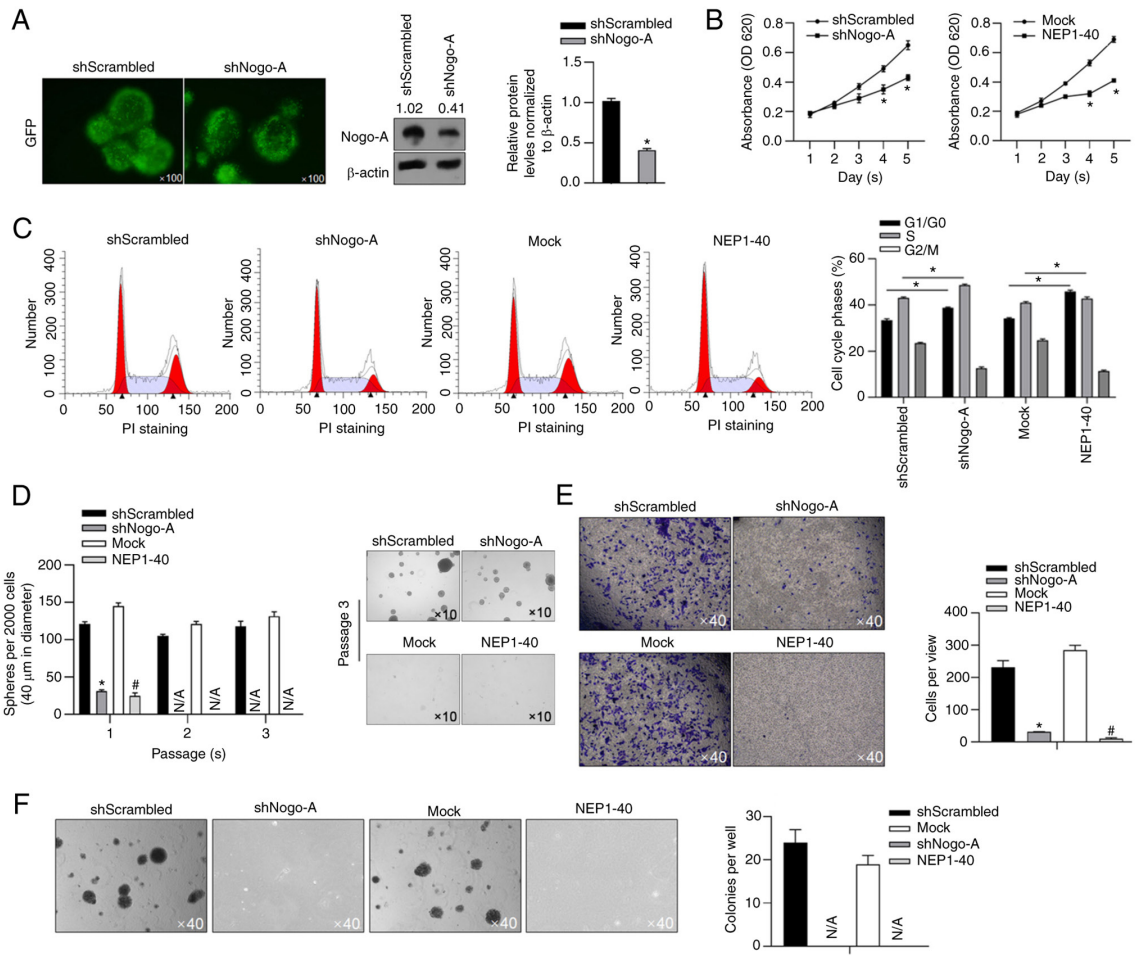

Figure 4. Nogo-A regulates malignant behaviors and stemness in U87-CSCs via Nogo-A/NgR signaling pathway. (A) GFP signal in vector was imaged to confirm the successful transfection of shScrambled or shNogo-A (left panel). Nogo-A was detected to confirm the knockdown efficacy of Nogo-A protein level (right panel). *P<0.05, vs. shScrambled. (B) After Nogo-A knockdown or inhibition of Nogo-A/NgR signaling pathway, cell viability from day 1 to 5 was measured by CCK-8. (C) Cell cycle distribution was measured by PI staining followed by flow cytometry. *P<0.05 vs. shScrambled; #P<0.05 vs. mock. (D) Serial replating assays were measured from passage 1 to 3. *P<0.05 vs. shScrambled; #P<0.05 vs. mock. (E) Transwell assays were performed. *P<0.05 vs. shScrambled. #P<0.05 vs. mock. (F) Tumor formation was performed in soft agar. GFP, green fluorescent protein; Nogo-A, neurite outgrowth inhibitor A; CCK-8, Cell Counting Kit-8; NgR, Nogo Receptor. CSCs, cancer stem cells; PI, propidium iodide.

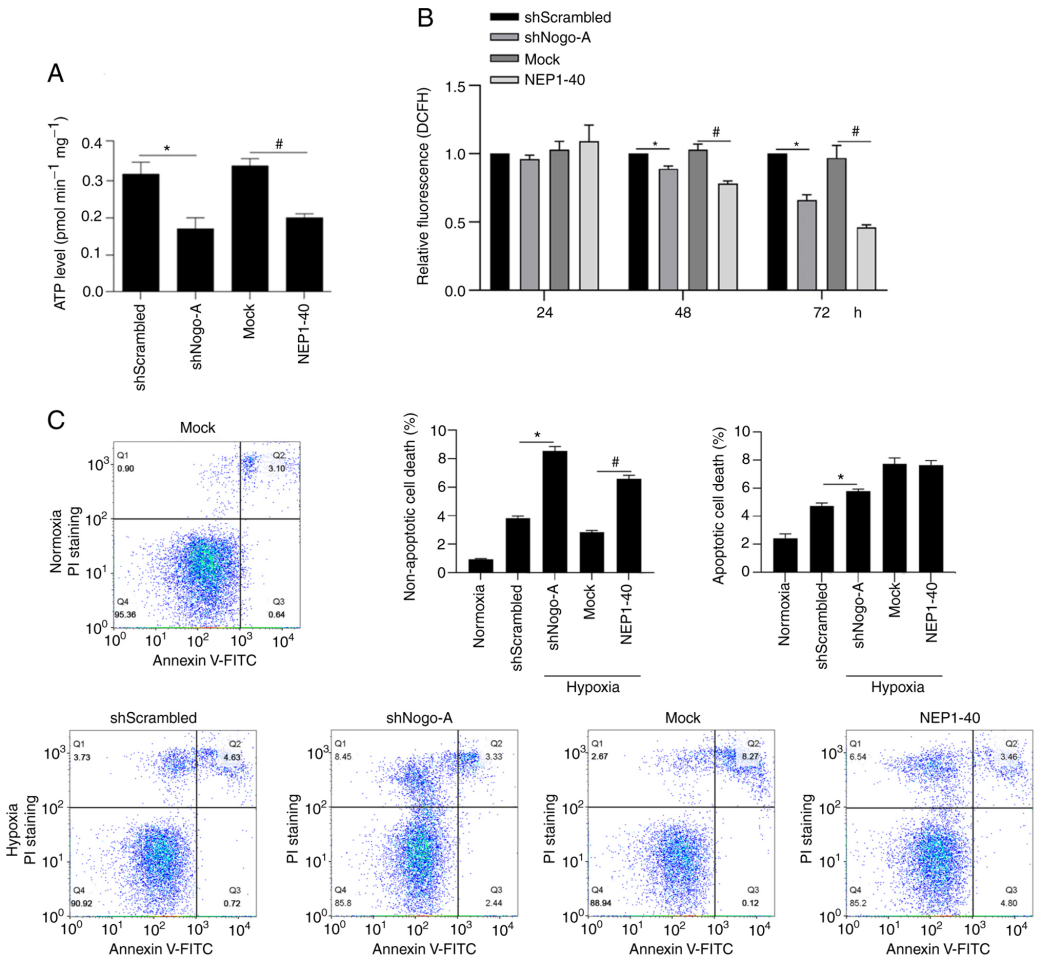

Figure 5. Nogo-A is related to mitochondrial function and protects U87MG-CSCs from hypoxia-induced cell death. (A) Synthesis of ATP under normoxia. *P<0.05 vs. shScrambled; #P<0.05 vs. mock. (B) ROS accumulation at 24, 48 and 72 h. *P<0.05 vs. shScrambled; #P<0.05 vs. mock. (C) Non-apoptotic cell death and apoptotic cell death levels were measured under hypoxic conditions by performing Annexin V-FITC and PI double staining. Quadrant 1 corresponds to non-apoptotic cell death; quadrants 2 and 3 correspond to apoptotic cell death. *P<0.05 vs. shScrambled/hypoxia group; #P<0.05 vs. mock/hypoxia group. Nogo-A, neurite outgrowth inhibitor A; PI, propidium iodide; DCFH, dichlorodihydrofluorescein.

Furthermore, Nogo-A was detected in U87MG and U87MG-CSCs from passage 1 to 4 by western blot analysis. As shown in Fig. 3B, stable expression levels of Nogo-A at all passages were observed in U87MG-CSCs, which were significantly higher than those in U87MG cells. After 5 and 10 days of differentiation, Nogo-A expression levels were significantly decreased, indicating that Nogo-A promotes stemness of CSCs derived from U87MG (Fig. 3C).

Nogo-A regulates malignant behaviors in U87MG-CSCs via interaction with NgR. Aiming to evaluate the effect of Nogo-A on malignant behaviors in U87MG-CSCs, Nogo-A was knocked down by transfecting Nogo-A targeting shRNA (shNogo-A), compared to negative control (shScrambled, Fig. 4A). Considering that the role of Nogo-A mainly is exerted by binding to NgR (20), NEP1-40, a competitive antagonist of the Nogo/NgR signaling pathway, was used to block Nogo-A activity (21). As shown in Fig. 4B, cell viability after days 4 and 5 was significantly inhibited by both Nogo-A knockdown and Nogo/NgR pathway inhibition by NEP1-40. Cell cycle distribution was then measured by performing PI staining followed by flow cytometry analysis. Moreover, the frequency of cells in the G_1 to G_0 phase of the cell cycle was significantly increased both by Nogo-A knockdown and Nogo/NgR signaling pathway inhibition using NEP1-40, indicating that cell proliferation was stimulated by Nogo-A via Nogo-A/NgR signaling pathway by promoting cell cycle entry (Fig. 4C). Using colony formation assays, it was observed that Nogo-A knockdown significantly decreased sphere formation, which is similar with the effect of addition of NEP1-40 in U87MG-CSCs (Fig. 4D). Other malignant behaviors were also assessed in U87MG-CSCs, including tumor formation and invasion in soft agar. As it is shown in Fig. 4E and F, Nogo-A knockdown or addition of NEP1-40 significantly decreased invasion and tumor formation capacities in U87MG-CSCs.

Nogo-A regulates ATP synthesis and ROS accumulation and exerts protective effect against hypoxia-induced cell death. It has been reported that hypoxia/reoxygenation-induced mitochondria-dependent apoptosis is tightly regulated by Nogo-A/NgR signaling pathway (22). This prompted us to determine whether Nogo-A/NgR signaling pathway is involved in mitochondrial energy metabolism. To achieve this goal, mitochondrial ATP synthesis, ROS accumulation and apoptosis were assessed. Firstly, ATP synthesis was measured following Nogo-A knockdown or Nogo-A/NgR signaling

pathway inhibition. Both approaches resulted in decreased intracellular ATP levels (Fig. 5A), indicating that Nogo-A/NgR signaling could promote metabolism. After 24-, 48- and 72-h inhibition of the Nogo-A/NgR signaling pathway, ROS accumulation was significantly decreased. This observation could be explained by a decrease in ATP synthesis and utilization with a concomitant decrease in ROS generation and accumulation (Fig. 5B). These results suggested that Nogo-A/NgR signaling could sensitize cells to hypoxia, which could induce ROS accumulation.

Moreover, cell death was detected in CSCs following hypoxia exposure. Hypoxia treatment notably increased apoptosis compared with normoxia group (Fig. 5C). Following Nogo-A knockdown or addition of NEP1-40, both non-apoptotic and apoptotic cell death were significantly increased. Interestingly, non-apoptotic cell death was increased by NEP1-40, whereas apoptotic cell death was not affected by NEP1-40. Taken together, these results indicated that Nogo-A/NgR signaling pathway tightly regulates hypoxia/reoxygenation-induced mitochondria-dependent apoptosis.

Discussion

In the present study, high levels of Nogo-A protein expression were observed in U87MG-CSCs, which decreased after CSC differentiation. Upregulated Nogo-A promoted the proliferation, entry into the cell cycle and tumor formation in soft agar in CSCs derived from U87MG cells. Although it is difficult to rule out the confounding effect of cell proliferation on cell invasion, invasiveness was also potentially enhanced in U87-CSCs compared to parental cells. Moreover, the effects of Nogo-A on these was dependent on its receptor, NgR. Knockdown of Nogo-A and inhibition of Nogo-A/NgR signaling pathway inhibited their roles in regulating CSCs. However, according to GEPIA database, no differences in Nogo-A expression levels were observed between glioblastoma tumor and adjacent tissues. These results indicated that Nogo-A could be expressed differently and serve different functions in CSCs, compared with parental glioblastoma cells.

Glioblastoma is the most common and fatal type of primary brain tumor due to the occurrence of chemoresistance and radioresistance (23), resulting in tumor growth, metastasis, and relapse (24,25). CSCs in glioblastoma are a sub-population emerging from the increased self-renewing division of glioblastoma cells or from the reprogramming of differentiated glioblastoma cells to undifferentiated forms (26). Thus, improving the understanding of the differences between CSCs derived from glioblastoma and their parental cells is of utmost importance to provide insights into strategies to overcome chemoresistance and radioresistance. Therefore, in the present study, CSCs were enriched from U87MG and their stemness was confirmed by detecting markers of stemness, including CD44 and CD133 (6). Self-renewal capacity was also assessed by performing serial replating assays, which is considered the gold standard of cell stemness detection. However, one limitation of this study is that additional experiments required to verify the CSC phenotype, such as RNA sequencing, were not performed.

Nogo-A was initially liked to the regulation of neurons in CNS (7,9,17) and, in recent years, accumulating evidence has emerged presenting its regulatory effects on the malignancy of glioblastoma cells (13,18,25). However, conflicting roles of Nogo-A in glioblastoma cells indicated that Nogo-A could exert complex functions under different conditions. The GEPIA server was used to determine the Nogo-A expression levels in different types of cancers and it was found that, except for pancreatic adenocarcinoma, no clear difference in Nogo-A expression was observed between tumor tissues and adjacent tissues, in agreement with the previous report (13). Instead of using clinical samples, CSCs were derived from U87MG glioblastoma cells and Nogo-A was upregulated compared with the parental cells. Moreover, after differentiation induced by culturing in serum-containing medium, a marked decrease in Nogo-A protein expression was observed in differentiated CSCs, further confirming the positive association between Nogo-A and stemness in CSCs derived from U87MG cells. As a limitation, however, the effect of the Nogo-A overexpression on the properties of CSCs could not be evaluated due to the relatively high endogenous Nogo-A expression level. In future studies, Nogo-A in U87MG glioblastoma cells overexpression may help confirm the alterations in the stemness of U87MG cells observed in the present study. The U87MG is widely used for investigating stemness of glioblastoma. However, as a limitation of the present study, only one source of CSCs was obtained from U87MG and more sources of CSCs are needed for further investigation.

CSCs derived from glioblastoma cells act differently, frequently promoting malignancies (4). The aim of this study was to determine whether Nogo-A was associated with malignancies in CSCs derived from glioblastoma cells. Nogo-A was knocked down by introducing shRNA targeting Nogo-A mRNA and the Nogo-A/NgR signaling pathway was blocked by adding NEP1-40, an antagonist of the Nogo-A/NgR signaling pathway (21). As expected, knockdown of Nogo-A and inhibition of the Nogo-A/NgR signaling pathway decreased malignant behavior, including cell proliferation, invasion and tumor formation in soft agar. Nogo-A/NgR signaling pathway was associated with the inhibition of the proliferation and differentiation in glioblastoma stem cells (27); however, in this study, following Nogo-A knockdown and Nogo-A/NgR pathway inhibition, the stemness of CSCs derived from U87MG glioblastoma cells were inhibited, which is in disagreement with the previous report (27). This could be due to the use of different CSCs enrichment methods, which could result in different sub-populations of CSCs.

It has been reported that, under hypoxic conditions, Nogo-A binds to Apg-1, a member of the stress-induced heat-shock protein of 110 kDa (Hsp110), and thus exerts a protective effect against hypoxia-induced cell death (28). Considering the regulatory role exerted by Nogo-A under hypoxic conditions, CSCs were also exposed to hypoxic conditions for 2 h to find out that a decrease in Nogo-A expression and the Nogo-A/NgR signaling pathway inhibition were associated with a decrease in mitochondrial ATP synthesis and ROS accumulation. Furthermore, non-apoptotic and apoptotic cell death were also increased in hypoxic conditions, indicating that in CSCs, Nogo-A could exert protective effects against hypoxia and oxidative stress. It was also hypothesized that altered mitochondrial functions, including ATP synthesis, could also affect malignant behaviors of CSCs in a Nogo-A/NgR signaling pathway related manner.

Nogo-A was upregulated in CSCs derived from glioblastoma and functioned as a key factor in promoting malignant

behaviors and protecting cells from exposure to hypoxic conditions. Moreover, it was found that Nogo-A critically regulated mitochondrial function, ATP synthesis, and maintenance of stemness via interacting with NgR. These data highlight Nogo-A as a potential therapeutic target for glioblastoma.

Acknowledgements

The authors would like to thank Dr Yin Li (Chongqing University) for language editing.

Funding

No funding was received.

Availability of data and materials

The datasets used and/or analyzed during the current study are available from the corresponding author on reasonable request.

Authors' contributions

CA, YuZ and YiZ designed the experiments and performed most of the experiments included in this study. CA, YuZ and KP performed cell culture, RNA isolation and protein extraction experiments. CA, YY and YiZ are responsible for data collection and performed statistical analysis. All authors read and approved the final manuscript. All authors confirm the authenticity of all the raw data.

Ethics approval and consent to participate

Not applicable.

Patient consent for publication

Not applicable.

Competing interests

The authors declare that they have no competing interests.

References

1. Mitre AO, Florian AI, Buruiana A, Boer A, Moldovan I, Soritau O, Florian SI and Susman S: Ferroptosis involvement in glioblastoma treatment. Medicina (Kaunas) 58: 319, 2022.
2. Wang Y and Jiang T: Understanding high grade glioma: Molecular mechanism, therapy and comprehensive management. Cancer Lett 331: 139-146, 2013.
3. Ramaswamy V and Taylor MD: The amazing and deadly glioma race. Cancer Cell 28: 275-277, 2015.
4. Alcantara Llaguno S and Parada LF: Cancer stem cells in gliomas: Evolving concepts and therapeutic implications. Curr Opin Neurol 34: 868-874, 2021.
5. Lathia JD, Mack SC, Mulkearns-Hubert EE, Valentim CL and Rich JN: Cancer stem cells in glioblastoma. Genes Dev 29: 1203-1217, 2015.
6. Seifert C, Balz E, Herzog S, Korolev A, Gaßmann S, Paland H, Fink MA, Grube M, Marx S, Jedlitschky G, *et al*: PIM1 inhibition affects glioblastoma stem cell behavior and kills glioblastoma stem-like cells. Int J Mol Sci 22: 11126, 2021.
7. GrandPré T, Nakamura F, Vartanian T and Strittmatter SM: Identification of the Nogo inhibitor of axon regeneration as a reticulon protein. Nature 403: 439-444, 2000.
8. Petrinovic MM, Duncan CS, Bourikas D, Weinman O, Montani L, Schroeter A, Maerki D, Sommer L, Stoeckli ET and Schwab ME: Neuronal Nogo-A regulates neurite fasciculation, branching and extension in the developing nervous system. Development 137: 2539-2550, 2010.
9. Mathis C, Schröter A, Thallmair M and Schwab ME: Nogo-a regulates neural precursor migration in the embryonic mouse cortex. Cereb Cortex 20: 2380-2390, 2010.
10. Schwab ME: Functions of Nogo proteins and their receptors in the nervous system. Nat Rev Neurosci 11: 799-811, 2010.
11. Xiong NX, Zhao HY, Zhang FC and He ZQ: Negative correlation of Nogo-A with the malignancy of oligodendroglial tumor. Neurosci Bull 23: 41-45, 2007.
12. Schwab DE, Lepski G, Borchers C, Trautmann K, Paulsen F and Schittenhelm J: Immunohistochemical comparative analysis of GFAP, MAP-2, NOGO-A, OLIG-2 and WT-1 expression in WHO 2016 classified neuroepithelial tumors and their prognostic value. Pathol Res Pract 214: 15-24, 2018.
13. Behling F, Barrantes-Freer A, Behnes CL, Stockhammer F, Rohde V, Adel-Horowski A, Rodríguez-Villagra OA, Barboza MA, Brück W, Lehmann U, *et al*: Expression of Olig2, nestin, NogoA and AQP4 have no impact on overall survival in IDH-wildtype glioblastoma. PLoS One 15: e229274, 2020.
14. Wang X, Zhou W, Li X, Ren J, Ji G, Du J, Tian W, Liu Q and Hao A: Graphene oxide suppresses the growth and malignancy of glioblastoma stem cell-like spheroids via epigenetic mechanisms. J Transl Med 18: 200, 2020.
15. Shtivelman E and Bishop J: Expression of CD44 is repressed in neuroblastoma cells. Mol Cell Biol 11: 5446-5453, 1991.
16. Nanduri LS, Maimets M, Pringle SA, van der Zwaag M, van Os RP and Coppes RP: Regeneration of irradiated salivary glands with stem cell marker expressing cells. Radiother Oncol 99: 367-372, 2011.
17. Wälchli T, Pernet V, Weinmann O, Shiu JY, Guzik-Kornacka A, Decrey G, Yüksel D, Schneider H, Vogel J, Ingber DE, *et al*: Nogo-A is a negative regulator of CNS angiogenesis. Proc Natl Acad Sci USA 110: E1943-E1952, 2013.
18. Wirthschaft P, Bode J, Soni H, Dietrich F, Krüwel T, Fischer B, Knobbe-Thomsen CB, Rossetti G, Hentschel A, Mack N, *et al*: RhoA regulates translation of the Nogo-A decoy SPARC in white matter-invading glioblastomas. Acta Neuropathol 138: 275-293, 2019.
19. Aldape K, Zadeh G, Mansouri S, Reifenberger G and von Deimling A: Glioblastoma: Pathology, molecular mechanisms and markers. Acta Neuropathol 129: 829-848, 2015.
20. Zagrebelsky M and Korte M: Maintaining stable memory engrams: New roles for Nogo-A in the CNS. Neuroscience 283: 17-25, 2014.
21. Fang Y, Yao L, Li C, Wang J, Wang J, Chen S, Zhou XF and Liao H: The blockage of the Nogo/NgR signal pathway in microglia alleviates the formation of Aβ plaques and tau phosphorylation in APP/PS1 transgenic mice. J Neuroinflammation 13: 56, 2016.
22. Sarkey JP, Chu M, McShane M, Bovo E, Ait Mou Y, Zima AV, de Tombe PP, Kartje GL and Martin JL: Nogo-A knockdown inhibits hypoxia/reoxygenation-induced activation of mitochondrial-dependent apoptosis in cardiomyocytes. J Mol Cell Cardiol 50: 1044-1055, 2011.
23. Lima FR, Kahn SA, Soletti RC, Biasoli D, Alves T, da Fonseca AC, Garcia C, Romão L, Brito J, Holanda-Afonso R, *et al*: Glioblastoma: Therapeutic challenges, what lies ahead. Biochim Biophys Acta 1826: 338-349, 2012.
24. Diaz A and Leon K: Therapeutic approaches to target cancer stem cells. Cancers (Basel) 3: 3331-3352, 2011.
25. Ortensi B, Setti M, Osti D and Pelicci G: Cancer stem cell contribution to glioblastoma invasiveness. Stem Cell Res Ther 4: 18, 2013.
26. Safa AR, Saadatzadeh MR, Cohen-Gadol AA, Pollok KE and Bijangi-Vishehsaraei K: Glioblastoma stem cells (GSCs) epigenetic plasticity and interconversion between differentiated non-GSCs and GSCs. Genes Dis 2: 152-163, 2015.
27. Meng Y, Shang F and Zhu Y: miR-124 participates in the proliferation and differentiation of brain glioma stem cells through regulating Nogo/NgR expression. Exp Ther Med 18: 2783-2788, 2019.
28. Kern F, Stanika RI, Sarg B, Offterdinger M, Hess D, Obermair GJ, Lindner H, Bandtlow CE, Hengst L and Schweigreiter R: Nogo-A couples with Apg-1 through interaction and co-ordinate expression under hypoxic and oxidative stress. Biochem J 455: 217-227, 2013.